Bulgarian Chemical Communications, Volume 50, Special Issue I (pp. 25 – 37) 2018

An entry to the synthesis of uleine-type alkaloids by Fischer indole synthesis reactions: FT-IR, NMR spectroscopy and computational study of the substituted carbazole compound

G. Serdaroglu[1], N. Uludag[2*]

[1]*Sivas Cumhuriyet University, Department of Science Education,58040,Sivas, Turkey*
[2]*Namık Kemal University, Department of Chemistry, 59030, Tekirdag, Turkey*

Received July 1, 2018; Accepted October 1, 2018

An efficient and straightforward method for the synthesis of 2-(2,3,4,9-tetrahydro-1*H*-carbazole-2-yl)acetonitrile by Fischer reaction of phenylhydrazine hydrochloride acid and 2-(3-oxocyclohexyl)acetonitrile in presence of ethanol is reported. Mild reaction conditions, good yields of products, short reaction times, and operational simplicity are the advantages of this procedure. PES scan was performed to determine the stable conformers of the studied compound in the gas phase at B3LYP/6-31G(d,p) level of the theory.The ^1H and ^1C NMR chemical shifts for each stable conformer of the studied compound were observed and simulated by the DFT method in both gas and water phases. Also, the recorded FT-IR spectrum of the studied compound wascompared with the simulated vibrational modes for each stable conformer. NBO was employed to predict the important intra-molecular interactions contributing to the lowering of the molecular stabilization energy of each stable conformer. FMO analysis and MEP diagrams were performed to predict the physicochemical and quantum chemical parameters to estimate the chemical reactivity behavior and reactive sites of each stable conformer.

Keywords: *Strychnos* alkaloids, FT-IR, NMR, FMO, NBO

INTRODUCTION

The natural carbazole ring skeleton of indole alkaloids often serves as a key intermediate for the synthesis of pentacyclic *strychnos* alkaloids. It is found in over 300 natural products belonging to several biogenetic types, and including two of the best-known alkaloids, uleine,anddasycarpidone [1, 2]. It has been greatly used in the synthesis of natural products (NP_s), as well as in medicinal chemistry [3]. Among them, uleine-type NP_s exhibit remarkable biological activities such as anti-ulcer [4] and acetylcholinesterase inhibitory activities, and further research toward their potential bioactivities is of current interest [5]. Accordingly, significant efforts have been devoted to the efficient synthesis of this type of alkaloids [6-8]. Recently, we have described the synthesis of the uleine-type alkaloids (Fig. 1) [9-13]. Efficient and atom-economic total synthesis of a complex molecule is a great endeavor in organic synthesis. Consequently, one step reactions have received much attention because they minimize the time and cost of the synthesis of highly functional molecules from simple building blocks. Moreover, this present method is advantageous with respect to the alternative synthetic approaches described for the synthesis of azocino [4,3-*b*] indole motif which is also found as a key feature in other *strychnos* alkaloids. It was decided to construct the 2-(2,3,4,9-tetrahydro-1*H*-carbazole-2-yl)acetonitrile of **3.** In this study, we present a new protocol for the enhanced construction of the skeleton toward the synthesis of uleine-type alkaloids.

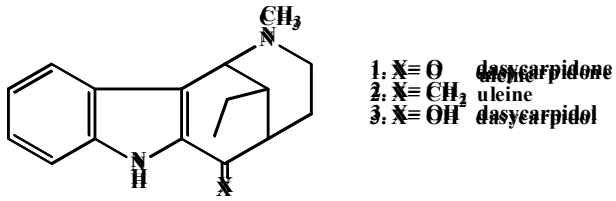

Fig. 1. Representatives of *uleine-type* alkaloids

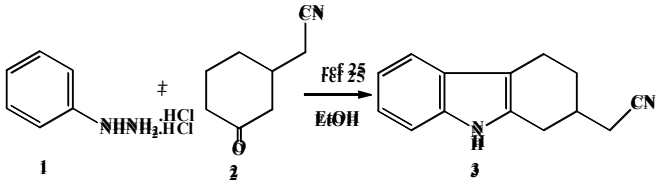

Scheme 1. Synthesis of 2-(2,3,4,9,-tetrahydro-1*H*-carbazol-2-yl)acetonitrile

* To whom all correspondence should be sent:
E-mail:nuludag@nku.edu.tr

EXPERIMENTAL AND COMPUTATIONAL DETAILS

^{1}H NMR (400 MHz) and ^{13}C NMR (100 MHz) spectra were recorded with a Bruker instrument DPX-400 MHz high-performancedigital FT-NMR spectrometer with $CDCl_3$ as the solvent and tetramethylsilane (TMS) as the internal standard at 25 ^{0}C. Chemical shifts are expressed in terms of parts per million (ppm) and the d coupling constants are given in Hz. IR spectra were obtained inKBr pellets using a Mattson 1000 FT-IR spectrometer. Elemental analyses were performed on a Costech ECS 4010analyzer. Melting points were determined in a capillary tube on a Gallenkamp apparatus and were uncorrected. Reactions were monitored by thin layer chromatography (silica gel60 F254). All reactions were carried out in an inert atmosphere of nitrogen. Purification of solvents was performed according to standard methods.

2-(2,3,4,9,-tetrahydro-1H-carbazol-2-yl)acetonitrile (3)

Phenylhydrazine hydrochloride (**1**) (3.00 g, 20.74 mmol) and 2-(3-oxocyclohexyl)acetonitrile [14] (**2**) (5.69 g, 41.48 mmol) were added to 250 mL of ethanol. The reaction flask was evacuated for 10 min and back-filled with dry nitrogen. The mixture was refluxed for 14 h under stirring. TLC indicated the end of the reaction and formation of the product. The mixture was cooled and then the mixture was evaporated *in vacuo*. The crude product was dissolved in chloroform and washed first with water (2×50 mL) and then with 100 mL of 10% NaOH solution. Following drying of the organic layer over $Na_2SO_4$the solvent was removed by evaporation and the residue was passed through a short silica gel column for further purification (1:1), ethyl acetate-*n*-hexane); R_f = 0.42) to give **3**. Yield 2.21 g(79%), as a pale yellow oil. IR (KBr, ν_{max}/cm^{-1}): 3267, 2925, 2165, 1607, 1455, 1319, 1241, 1010; ^{1}H NMR (400 MHz, CDCl3, δ/ppm): 7.77 (s, 1H), 7.45 (d, *J* = 6.7 Hz, 1H),), 7.34 (t, *J* = 8.0 Hz, 1H), 7.24 (td, *J* = 7.4 and 1.8 Hz, 1H), 2.94 (dd, *J* = 15.43 and 5.11 Hz, 1H), 2.77 (m, 2H), 2.62 (m, 1H), 2.54 (d, *J* = 7,4 and 3.8 Hz, 2H), 2.23 (m, 1H), 2.41 8m, 1H), 1.83 (m, 1H); ^{13}CNMR (100MHz,CDCl3,δ/ppm): 135.9, 131.6, 127.4, 121.4, 119.3, 119.9, 118.1, 111.2, 108.9, 32.1, 28.9, 28.1, 22.8, 19.3; Anal. Calc. for C_{14} H_{14} N_2: C, 79.96; H, 6.71; N, 13.32. Found: C, 79.91 ; H, 6.67 ;N, 13.37.

Computational details

The conformational analysis of the 2-(2,3,4,9-tetrahydro-1*H*-carbazol-2-yl)acetonitrile compound was employed to determine the stable conformer sat B3LYP/6-31G(d,p) level of the theory[16-17].Then, the three stable conformers predicted from the PES (potential energy surface) scan were re-optimized at 6-311++G(d,p) basis set in gas and water phase. The polarized continuum model (PCM) [18-19] was used to perform all analysessimulated in the water phase. NBO (natural bond orbital) analysis [20, 21] was conducted to elucidate the important intra-molecular interactions occurring in each stable conformer. The GIAO (Gauge-Independent Atomic Orbital) [22, 23] approach was used to predict the isotropic chemical shifts of each stable conformer. The simulated vibrational frequencies of each stable conformer were scaled down by using a scaling factor of 0.9668 [24] for B3LYP/6-311++G(d, p) and were assigned by VEDA package [25]. All calculations werecarried out by G09W [26] and all schemes were prepared by using the ChemOffice17 Suite [27]. GaussView 6.0 [28] was used to illustrate the HOMO, LUMO amplitudes and MEP diagrams, as well as to verify the vibrational modes of the stable conformers.

RESULTS AND DISCUSSION

In this study,our goal was to simplify the synthesis of compound **3** and we applied a new synthetic route for the synthesis of 2-(2,3,4,9,-tetrahydro-1*H*-carbazol-2-yl)acetonitrile in high yields (up to 76%) through the indolization reaction between the starting phenylhydrazine hydrochloride and 2-(3-oxocyclohexyl)acetonitrile (**2**), which has been previously synthesized [14]. Reaction of compound **2** with phenylhydrazine hydrochloride by the Fischer indole reaction gave the carbazole derivative **3**. This compound is a versatile synthetic block and a subgroup of the uleine-type skeleton. 2-(2,3,4,9,-tetrahydro-1*H*-carbazol-2-yl) acetonitrile moiety bearing a nitrile chain at the bridge carbon atom is the common key structure of the uleine alkaloids (Scheme 1) [15]. The basic skeletal features of these compounds, particularly pentacyclic ABCDE framework, can be seen in the namesake of the uleine family. In this study, new methodologies combining operational simplicity, high yields, readily available starting materials and low-cost reagents are desirable for the high throughput preparation of the target compounds.

Conformational analysis and structure descriptions

Fig.2 shows the structural skeleton with the original atomic numbers and ring descriptions of the 2-(2,3,4,9-tetrahydro-1*H*-carbazol-2-yl) acetonitrile compound. According to the acetonitrile group rotation around the ring part of the studied compound, one-dimensional PES scan (1D-PES) analysis was conducted by varying the dihedral angle τ (C27-C26-C13-C12) in the range of 0^0- 360^0 in steps of $10^0$to predict the stable conformers in the gas phase by the B3LYP/6-31G(d,p) level of the theory. Fig.3 shows three stable conformers determined at -63^0, 67^0 and 188^0 dihedral angles. All re-optimized conformers having no imaginary frequency wereproved*via* conducting frequency calculations at 6-31G(d,p) and 6-311++G(d,p) basis sets in both gas and water phase. Table 1 shows the total and relative energy values for the three stable conformers, whose relative energies are close to each other and vary between 0-3.58 kcal mol^{-1} for the 6-311++G(d,p) basis set (gas phase). It is clear that Conf3 is the most stable conformer except for the water phase by 6-311++G(d,p) basis set. On the other hand, Conf1 is predicted as the most stable conformer in the water phase by 6-311++G(d,p) basis set even though the energies of the Conf1 and Conf3 are very close to each other.

The selected optimized geometries of each stable conformer are given in Table 2 and are compared with the geometric parameters of the structurally related carbazole compound [29]because of lack of experimental and computational data. From Table 2, it can be seen that the bond lengths and angles for the three stable conformers are calculated to be very close to each other and the non-bonding angles for these conformers are different from each other. The C1-C2 and C4-C5 bond lengths belonging to the aromatic ring (R**A)** for all conformers were determined in the range of 1.41-1.43Å and were observed in the range of 1.39-1.41 Å[29]. Also, the C4-N23 bond length for the stable conformers is the same as each other, that is, this bond length has been predicted in 1.38 Å and was observed in 1.37 Å[29]. Similarly, the bond angles for each stable conformer are almost similar: the bond angles for all stable conformers were determined at C2-C1-C6=121^0, C3-C4-C23= 131^0, C5-C4-C23=107^0, and C11-C12-C13=110^0, and there is very good agreement with the corresponding experimental ones. On the other hand, the non-bonding angles have considerably varied from each other according to the acetonitrile group position around the ring part of the compound. The non-bonding angle C27-C26….C11 for the Conf1, Conf2 and Conf3 was calculated as 149^0, 75^0, 112^0 respectively. Here, it should be seen that the non-bonding angle for the Conf2 is smaller than that of the other conformers because the acetonitrile group for Conf2 is folded over the R**C** (ring **C**) more than the other conformers. Furthermore, the dihedral angles for the aromatic part of all stable conformers were computed as follows: C1-C2-C3-C4=0^0, C4-C5-C6-C1=0^0, N23-NC4-C3-C2=180^0, N23C11-C16-C5= 0^0 and agree with the corresponding observed ones. Moreover, the dihedral angle C27-C26-C13-C12 for the stable conformers was calculated as 177^0 (Conf1), -55^0 (Conf2), 66^0 (Conf3). From Table 2, it is clear that the acetonitrile group for Conf1 is a little deviated (3^0) from C27-C26-C13-C12 backbone plane. The dihedral angle C12-C13-C14-C15 for the non-aromatic part of each stable conformer was predicted as 61^0 (Conf1), 57^0 (Conf2), 61^0 (Conf3) which are very close to the observed 62^0.

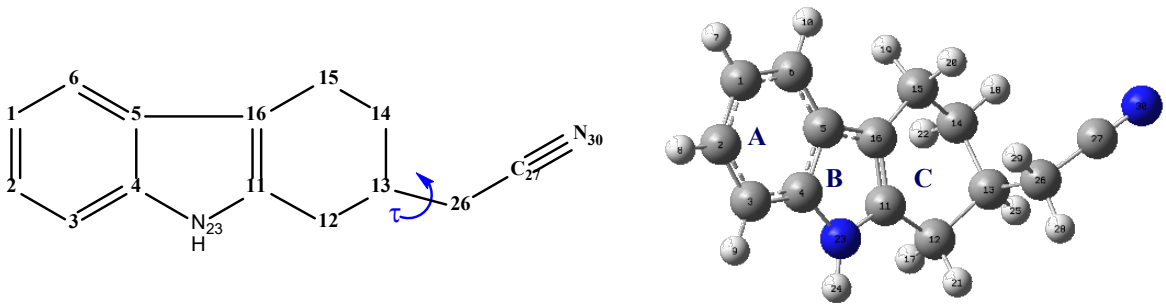

Fig. 2. The 2-(2,3,4,9-tetrahydro-1*H*-carbazol-2-yl)acetonitrile compound with the ring definition (right) and the skeleton of the compound with dihedral angle (left) τ (C27-C26-C13-C12)

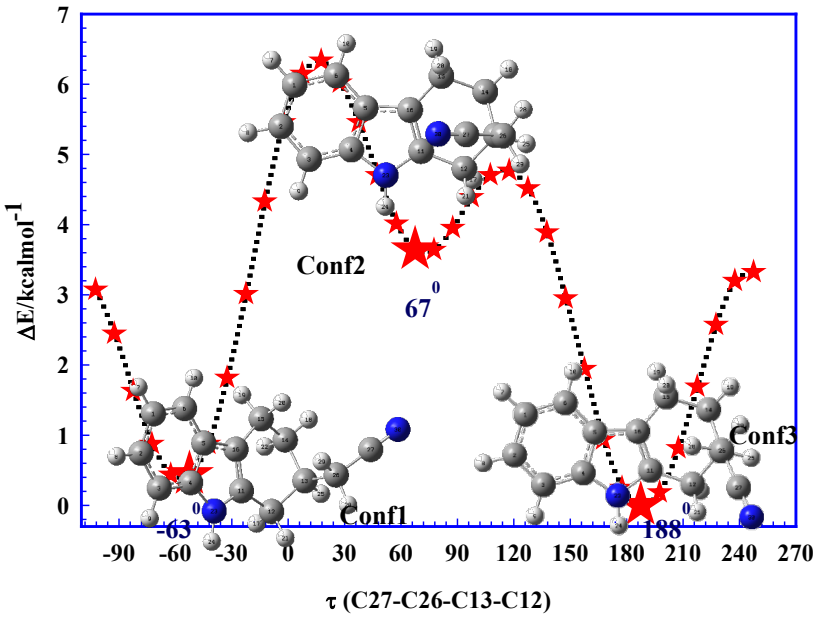

Fig. 3. PES scan of the studied compound at the B3LYP/6-31G(d,p) level of the theory in the gas phase.

Table 1. Total and relative energies for the three stable conformers of the studied compound.

Conf.	6-31G(d,p)				6-311++G(d,p)			
	Tot. energy/ hartree	ΔE/ kcalmol^{-1}	Free energy / hartree	ΔG/ kcalmol^{-1}	Tot. energy / hartree	ΔE / kcalmol^{-1}	Free energy / hartree	ΔG / kcalmol^{-1}
Gas Phase								
Conf1	-651.451845	0.366528	-651.241072	0.311245	-651.598189	0.384437	-651.388981	0.291792
Conf2	-651.446696	3.597769	-651.236057	3.458205	-651.592778	3.779973	-651.383752	3.573039
Conf3	-651.452430	0.000000	-651.241568	0.000000	-651.598802	0.000000	-651.389446	0.000000
Water phase								
Conf1	-651.464982	0.030980	-651.254216	0.020080	-651.612760	0.060856	-651.403627	0.000000
Conf2	-651.461789	2.034687	-651.250881	2.112824	-651.609383	2.180006	-651.399905	2.335590
Conf3	-651.465031	0.000000	-651.254248	0.000000	-651.612857	0.000000	-651.403603	0.015060

Table 2. Selected structural parameters for the three conformers of the studied compound at B3LYP/6-311++G(d,p) in the water phase

Bond Length (Å)	Exp.	Conf1	Conf2	Conf3	*Non-bonding angle (^{0})*	Exp.	Conf1	Conf2	Conf3
C1-C2	1.39[a]	1.41	1.41	1.41	C27-C26….C11		149	75	112
C4-N23	1.37[a]	1.38	1.38	1.38	C27-C26….C12		148	96	97
C4-C5	1.41[a]	1.43	1.43	1.43	C27-C26….C14		94	105	147
C11-C16	1.36[a]	1.37	1.37	1.37	C27-C26….C15		102	77	160
C11-N23	1.38[a]	1.38	1.38	1.38	N30-C27….C11		159	103	132
N23-H24	0.86[a]	1.00	1.00	1.00	N30-C27….C12		159	126	124
C27-N30		1.15	1.15	1.15	N30-C27….C14		123	133	158
C26-C27		1.46	1.46	1.46	N30-C27….C15		125	106	166
Bond angle (^{0})					*Dihedral angle (^{0})*				
C2-C1-C6	121[a]	121	121	121	C1-C2-C3-C4	0.0[a]	0	0	0
C3-C4-N23	131[a]	131	131	131	C4-C5-C6-C1	0.6[a]	-0	-0	-0
C5-C4-N23	107[a]	107	107	107	N23-C4-C3-C2	180.0[a]	180	180	180
C4-N23-H24	125[a]	126	126	126	N23-C11-C16-C5	0.8[a]	0	0	0
C12-C13-C14	113[a]	110	111	111	N30-C27-C26-C13		-54	163	28
C26-C27-N30		179	177	179	C27-C26-C13-C12		177	-55	66
C14-C15-C16	110[a]	111	110	111	C27-C26-C13-C14		-60	74	-171
C14-C13-C26		113	113	110	C12-C13-C14-C15	62.0^0	61	57	61
C11-C12-C13	111[a]	110	110	110	C12-C11-C16-C15	0.2^0	-1	-2	-1

*experimental data are taken from ref.[29]

NBO analysis

NBO analysis [20,21] was used to elucidate the important intra-molecular interactions such as resonance and hyper conjugative interactions contributing to the lowering of the stabilization

energy of a molecular system by using the results of the second order perturbative theory analysis.

Table 3 shows selected results obtained from the second order perturbative theory analysis for the three stable conformers at B3LYP/6-311++G(d,p) level in the water phase. Accordingly, the interaction energies occurred in the aromatic part of each stable conformers are very close to each other: the stabilization energy for the resonance interaction between the filled orbital π (C1-C2) and theunfilled orbital π (C3-C4) are calculated as Conf1=9.45, Conf2=9.47, Conf3=9.43 kcalmol^{-1}. In addition, the other resonance energies for the π (C3-C4)→ π *(C1-C2) and π (C3-C4)→ π *(C5-C6) interactions are computed as 5.35 and 8.21 kcal mol^{-1} for Conf1; 4.65 and 8.76 kcalmol^{-1} for Conf2; 5.76 and 8.18 kcalmol^{-1} for Conf3.It should be noticed, however, that the stabilization energy of the interaction π (C11-C12)→ π* (C5-C6) occurred in the R**B** of each stable conformer was computed as 9.91 kcalmol^{-1} for Conf1, 12.01 kcal mol^{-1} for Conf2, 9.93 kcalmol^{-1} for Conf3. Here, it is clear from Table 3 that the stabilization energies occurring in the non-aromatic part of each stable conformer have begun to differ from each other according to the acetonitrile group orientation. In addition, there are also hyper-conjugative interactions being important for the stabilization energy, that is, the stabilization energies of the intra-molecular charge transfer for σ C12-H17→ π* (C11-C16)were calculated as 2.40 kcalmol^{-1} for Conf1 and Conf3, 2.41 kcalmol^{-1} for Conf2. On the other hand, the resonance energiesof the interactions π (C27-N30)→ π* (C1-C2) and π (C27-N30)→ π* (C5-C6) occurring between the nitrile group and the aromatic ring were calculated as 0.37 kcalmol^{-1}for Conf1 and 17.44 kcalmol^{-1} for Conf2, but this kind of interaction was not determined for Conf3. It is clear that when the stabilization energies of LP (1) N23 and LP (1) N30 are compared with each other, the interaction energy between LP (1) N23 and the antibonding orbital is higher than that of LP (1) N30: the stabilization energies for the LP(1) N23→ π* (C3-C4) and LP(1) N30→ π* (C26-C27) interactions are calculated as 20.24 kcalmol^{-1} and 4.90 kcalmol^{-1} for Conf1, 19.78 kcalmol^{-1} and 3.37 kcalmol^{-1} for Conf2, 20.21 kcalmol^{-1} and 5.22 kcalmol^{-1} for Conf3, respectively. It can be said that the important contribution to the lowering of the molecular stabilization energy was provided by the intra-molecular charge transfer from the lone pair of the N23 atom to antibonding orbital(s), more than the lone pair of N30 atom.

Global reactivity parameters, FMO (Frontier Molecular Orbital) analysis and MEP (Molecular Electrostatic Potential)

FMO analysis is a very useful tool to explain/ elucidate the kinetic stability, chemical reactivity behavior *via* the HOMO and LUMO orbitals showing the nucleophilic and electrophilic character of a sample molecular system. As it is well known, the ionization energy (*I*) and electron affinity (*A*) can be obtained from the HOMO and LUMO orbital energies according to the Koopman's theorem [30]. In addition, Parr and co-workers [31] have defined the DFT-based reactivity descriptors that are the electronic chemical potential (χ), global hardness (η), electrophilicity (ω) and the maximum charge transfer index (ΔNmax) as shown below:

$$I = -E_{HOMO} \quad (1)$$

$$A = -E_{LUMO} \quad (2)$$

$$\chi = -\frac{I+A}{2} \quad (3)$$

$$\eta = \frac{I-A}{2} \quad (4)$$

$$\omega = \frac{\mu^2}{2\eta} \quad (5)$$

$$\Delta N_{max} = \frac{I+A}{2(I-A)} \quad (6)$$

Table 4 presents the quantum chemical identifiers of each stable conformer of the studied compound obtained from the equations given above. The energy gap (ΔE) has changed in the following order: Conf2< Conf1< Conf3 in both the gas and water phases at two basis sets. It is clear that Conf2 has the lowest ΔE value which means the highest chemical reactivity and lowest kinetic stability. Moreover, the global hardness (η) has changed as Conf2< Conf1< Conf3 similar to the energy gap ordering of the stable conformers, in both the gas and water phases at two basis sets. Here, it can be noticed that Conf2 has the lowest hardness value which makes it the soft conformer of the studied compound. If it is looked at the chemical potential ordering of the three conformers, it can be seen that it has changed as Conf1< Conf3< Conf2. It can be also seen that Conf1 is the best electrophile because the electrophilicity index has changed as Conf2< Conf3< Conf1, in both the gas and water phases at two basis sets. But the maximum charge transfer capability (ΔNmax) calculated in the different ordering based on the basis set: (ΔNmax) has changed as Conf2< Conf3< Conf1 at 6-31G(d,p) basis set in both phases while it has changed as Conf3< Conf1< Conf2 at 6-311++G(d,p) basis set in both phases.

Table 3. Second-order perturbation theory analysis of the Fock matrix in NBO basis for the three stable conformers at B3LYP/6-311++G(d,p) level of the theory in the water phase

Donor(i)	Hybridization	ED_i/e	Acceptor (j)	Hybridization	ED_j/e	E(2)/ kcalmol^{-1}	E(j)-E(i)/ a.u	F(i.j)/ a.u
Conf1								
πC1-C2 (2)	0.7099 $p_{(C1)}$+ 0.7043 $p_{(C2)}$	0.82922	π* C3-C4	$p_{(C3)}$- $p_{(C4)}$	0.21516	9.45	0.27	0.066
			π* C5-C6	$p_{(C5)}$- $p_{(C6)}$	0.22349	9.83	0.28	0.069
π C3-C4 (2)	0.7117 $p_{(C3)}$+ 0.7025 $p_{(C4)}$	0.81948	π* C1-C2	$p_{(C1)}$- $p_{(C2)}$	0.21085	5.35	0.55	0.070
			π* C5-C6	$p_{(C5)}$- $p_{(C6)}$	0.22349	8.21	0.29	0.063
π C5-C6 (2)	0.7182 $p_{(C5)}$+ 0.6958 $p_{(C6)}$	0.81161	π* C1-C2	$p_{(C1)}$- $p_{(C2)}$	0.21085	5.22	0.54	0.068
			π* C3-C4	$p_{(C3)}$- $p_{(C4)}$	0.21516	9.98	0.27	0.067
			π* C11-C16	$p_{(C11)}$- $p_{(C16)}$	0.15476	7.45	0.29	0.060
πC11-C16 (2)	0.6871 $p_{(C11)}$+ 0.7266 $p_{(C16)}$	0.91108	π* C5-C6	$p_{(C5)}$- $p_{(C6)}$	0.22349	9.91	0.30	0.073
			π* C11-C16	$p_{(C11)}$- $p_{(C16)}$	0.15476	0.55	0.31	0.017
σC12-H17 (1)	0.7831 $sp^{3.55}{}_{(C12)}$+ 0.6219 $s_{(H17)}$	0.98233	π* C11-C16	$p_{(C11)}$- $p_{(C16)}$	0.15476	2.40	0.55	0.049
σC12-H21 (1)	0.7817 $sp^{3.43}{}_{(C12)}$+ 0.6237 $s_{(H21)}$	0.98722	π* C11-C16	$p_{(C11)}$- $p_{(C16)}$	0.15476	1.08	0.55	0.033
σC15-H20 (1)	0.7767 $sp^{3.57}{}_{(C15)}$+ 0.6299 $s_{(H20)}$	0.98565	π* C11-C16	$p_{(C11)}$- $p_{(C16)}$	0.15476	2.11	0.54	0.046
πC27-N30 (3)	0.6590 $p_{(C27)}$+ 0.7521 $p_{(N30)}$	0.99423	π* C1-C2	$p_{(C1)}$- $p_{(C2)}$	0.21085	0.37	0.66	0.022
LP (1) N23	p	0.81653	π* C3-C4	$p_{(C3)}$- $p_{(C4)}$	0.21516	20.24	0.29	0.098
			π* C11-C16	$p_{(C11)}$- $p_{(C16)}$	0.15476	18.26	0.31	0.096
LP (1) N30	$sp^{0.92}$	0.98484	π* C26-C27	$sp^{2.93}{}_{(C26)}$- $sp^{0.86}{}_{(C27)}$	0.01081	4.90	0.98	0.088
Conf2								
πC1-C2 (2)	0.7100 $p_{(C1)}$+ 0.7042 $p_{(C2)}$	0.82977	π* C3-C4	$p_{(C3)}$- $p_{(C4)}$	0.21596	9.47	0.28	0.066
			π* C5-C6	$p_{(C5)}$- $p_{(C6)}$	0.21961	9.68	0.29	0.068
π C3-C4 (2)	0.7109 $p_{(C3)}$+ 0.7033 $p_{(C4)}$	0.82060	π* C1-C2	$p_{(C1)}$- $p_{(C2)}$	0.21099	4.65	0.65	0.071
			π* C5-C6	$p_{(C5)}$- $p_{(C6)}$	0.21961	8.76	0.30	0.066
π C5-C6 (2)	0.7107 $p_{(C5)}$+ 0.7035 $p_{(C6)}$	0.80662	π* C1-C2	$p_{(C1)}$- $p_{(C2)}$	0.21099	4.45	0.64	0.068
			π* C3-C4	$p_{(C3)}$- $p_{(C4)}$	0.21596	9.89	0.27	0.066
			π* C11-C16	$p_{(C11)}$- $p_{(C16)}$	0.15494	7.32	0.29	0.059
πC11-C16 (2)	0.6864 $p_{(C11)}$+ 0.7272 $p_{(C16)}$	0.91133	π* C5-C6	$p_{(C5)}$- $p_{(C6)}$	0.21961	12.01	0.30	0.081
			π* C11-C16	$p_{(C11)}$- $p_{(C16)}$	0.15494	0.52	0.30	0.016
σC12-H17 (1)	0.7832 $sp^{3.56}{}_{(C12)}$+ 0.6218 $s_{(H17)}$	0.98260	π* C11-C16	$p_{(C11)}$- $p_{(C16)}$	0.15494	2.41	0.55	0.049
σC12-H21 (1)	0.7816 $sp^{3.44}{}_{(C12)}$+ 0.6238 $s_{(H21)}$	0.98679	π* C5-C6	$p_{(C5)}$- $p_{(C6)}$	0.21961	0.50	0.54	0.023
			π* C11-C16	$p_{(C11)}$- $p_{(C16)}$	0.15494	1.20	0.55	0.035
σC15-H20 (1)	0.7773 $sp^{3.54}{}_{(C15)}$+ 0.6291 $s_{(H20)}$	0.98538	π* C5-C6	$p_{(C5)}$- $p_{(C6)}$	0.21961	1.87	0.53	0.045
			π* C11-C16	$p_{(C11)}$- $p_{(C16)}$	0.15494	2.17	0.54	0.046

πC26-C27 (1)	0.7066 $sp^{2.89}_{(C26)}$+ 0.7076 $sp^{0.86}_{(C27)}$	0.99387	π* C1-C2	$p_{(C1)}$- $p_{(C2)}$	0.21099	0.33	1.12	0.027
			π* C5-C6	$p_{(C5)}$- $p_{(C6)}$	0.21961	0.31	0.77	0.022
σC26-H28 (1)	0.7911 $sp^{3.46}_{(C26)}$+ 0.6117 $s_{(H28)}$	0.97813	π* C5-C6	$p_{(C5)}$- $p_{(C6)}$	0.21961	1.65	0.56	0.043
πC27-N30 (1)	0.6481 $sp^{1.15}_{(C27)}$+ 0.7616 $sp^{1.07}_{(N30)}$	0.99818	π* C1-C2	$p_{(C1)}$- $p_{(C2)}$	0.21099	4.98	1.45	0.121
πC27-N30 (2)	0.6569 $p_{(C27)}$+ 0.7540 $p_{(N30)}$	0.99434	π* C5-C6	$p_{(C5)}$- $p_{(C6)}$	0.21961	17.44	0.32	0.106
πC27-N30 (3)	0.6609 $p_{(C27)}$+ 0.7505 $p_{(N30)}$	0.99377	π* C5-C6	$p_{(C5)}$- $p_{(C6)}$	0.21961	2.44	0.40	0.044
LP (1) N23	p	0.81759	π* C3-C4	$p_{(C3)}$- $p_{(C4)}$	0.21596	19.78	0.29	0.098
			π* C11-C16	$p_{(C11)}$- $p_{(16)}$	0.15494	19.04	0.31	0.099
LP (1) N30	$sp^{0.92}$	0.98441	σ* C26-C27	$sp^{2.89}_{(C26)}$- $sp^{0.86}_{(C27)}$	0.01272	3.37	0.92	0.070
Conf3								
πC1-C2 (2)	0.7099 $p_{(C1)}$+ 0.7043 $p_{(C2)}$	0.82923	π* C3-C4	$p_{(C3)}$- $p_{(C4)}$	0.21517	9.43	0.28	0.066
			π* C5-C6	$p_{(C5)}$- $p_{(C6)}$	0.22352	9.84	0.28	0.069
π C3-C4 (2)	0.7117 $p_{(C3)}$+ 0.7025 $p_{(C4)}$	0.81943	π* C1-C2	$p_{(C1)}$- $p_{(C2)}$	0.21090	5.76	0.55	0.072
			π* C5-C6	$p_{(C5)}$- $p_{(C6)}$	0.22352	8.18	0.29	0.063
π C5-C6 (2)	0.7182 $p_{(C5)}$+ 0.6959 $p_{(C6)}$	0.81165	π* C1-C2	$p_{(C1)}$- $p_{(C2)}$	0.21090	5.26	0.53	0.068
			π* C3-C4	$p_{(C3)}$- $p_{(C4)}$	0.21517	9.96	0.27	0.067
			π* C11-C16	$p_{(C11)}$- $p_{(C16)}$	0.15472	7.45	0.29	0.060
πC11-C16 (2)	0.6869 $p_{(C11)}$+ 0.7267 $p_{(C16)}$	0.91124	π* C5-C6	$p_{(C5)}$- $p_{(C6)}$	0.22352	9.93	0.30	0.073
			π* C11-C16	$p_{(C11)}$- $p_{(C16)}$	0.15472	0.55	0.31	0.017
σC12-H17 (1)	0.7832 $sp^{3.54}_{(C12)}$+ 0.6218 $s_{(H17)}$	0.98256	π* C11-C16	$p_{(C11)}$- $p_{(C16)}$	0.15472	2.40	0.55	0.049
σC12-H21 (1)	0.7818 $sp^{3.42}_{(C15)}$+ 0.6235 $s_{(H21)}$	0.98682	π* C11-C16	$p_{(C11)}$- $p_{(C16)}$	0.15472	1.08	0.55	0.033
σC15-H19 (1)	0.7799 $sp^{3.49}_{(C15)}$+ 0.6259 $s_{(H19)}$	0.98692	π* C11-C16	$p_{(C11)}$- $p_{(C16)}$	0.15472	1.21	0.54	0.035
σC15-H20 (1)	0.7768 $sp^{3.57}_{(C15)}$+ 0.6298 $s_{(H20)}$	0.98566	π* C11-C16	$p_{(C11)}$- $p_{(C16)}$	0.15472	2.11	0.54	0.046
LP (1) N23	p	0.81646	π* C3-C4	$p_{(C1)}$- $p_{(C2)}$	0.21517	20.21	0.29	0.098
			π* C11-C16	$p_{(C11)}$- $p_{(C16)}$	0.15472	18.25	0.31	0.096
LP (1) N30	$sp^{0.92}$	0.98481	σ* C26-C27	$sp^{2.93}_{(C26)}$- $sp^{0.86}_{(C27)}$	0.01076	5.22	1.01	0.092

*E(2) stabilization energy; *εi,* and *εj* are diagonal elements, and *Fij* is the off-diagonal NBO Fock matrix element.

Fig. 4 presents the HOMO and LUMO visualization of all conformers by using the B3LYP/6-311++G(d,p) level of the theory in the water phase. From Fig.4 it can be seen that the HOMO is mainly localized on the aromatic part (R**A** and R**B**) and partly on the C12 and C15 atoms on the non-aromatic ring (R**C**) for all stable conformers. It can be said that the nucleophilic site for all stable conformers is around the R**A**, R**B**, and partly R**C**. It is clear that the electrophilic site is around the aromatic part and the C12 atom for all stable conformers. The MEP diagrams can be also used to illustrate the electrophilic and nucleophilic attack sites of the sample molecular system, as well as to predict the H-bonding tendency, chemical reactivity behavior of the biologically or pharmaceutically important molecules. Fig. 5 shows the MEP diagrams for all stable conformers in the water phase at 6-311++G(d,p) basis set. The electrostatic potential based on the total electron density surface of the stable conformers has changed as follows: Conf2 (±0.107e) = Conf3 (±0.107e) < Conf1 (±0.117e). Also, the color scheme indicates the electron poor (blue color) and electron rich (red color) region of the sample molecular system. It is clearly seen that the red color on the Conf2 is darker than that of the other conformers due to the possibility of intra-molecular charge transferbetween the acetonitrile group and the ring part of this conformer.

Table 4. The quantum chemical and physicochemical identifiers of the three stable conformers

Conformer		E_{HOMO}	E_{LUMO}	ΔE	μ	η	ω	ΔNmax
					6-31G(d,p)			
Conf1	Gas	-0.19874	-0.00848	5.17724	-2.81937	2.58862	1.53535	1.08914
Conf2	Gas	-0.19001	-0.00070	5.15139	-2.59474	2.57570	1.30697	1.00740
Conf3	Gas	-0.19805	-0.00743	5.18704	-2.79570	2.59352	1.50682	1.07796
					6-311++G(d,p)			
Conf1	Gas	-0.21130	-0.02615	5.03819	-3.23067	2.51910	2.07163	1.28247
Conf2	Gas	-0.20242	-0.02753	4.75900	-3.12863	2.37950	2.05680	1.31483
Conf3	Gas	-0.21059	-0.02543	5.03846	-3.21122	2.51923	2.04664	1.27468
					6-31G(d,p)			
Conf1	Water	-0.19667	-0.00848	5.12091	-2.79121	2.56046	1.52138	1.09012
Conf2	Water	-0.19524	-0.00811	5.09207	-2.76672	2.54603	1.50327	1.08668
Conf3	Water	-0.19665	-0.00829	5.12554	-2.78835	2.56277	1.51690	1.08802
					6-311++G(d,p)			
Conf1	Water	-0.20829	-0.02519	4.98241	-3.17666	2.49120	2.02536	1.27515
Conf2	Water	-0.20706	-0.02506	4.95247	-3.15816	2.47624	2.01393	1.27538
Conf3	Water	-0.20829	-0.02502	4.98703	-3.17435	2.49352	2.02053	1.27304

*ΔE (Energy Gap), χ,η, ω and $\Delta Nmax$ are in eV; HOMO and LUMO energies are in au.

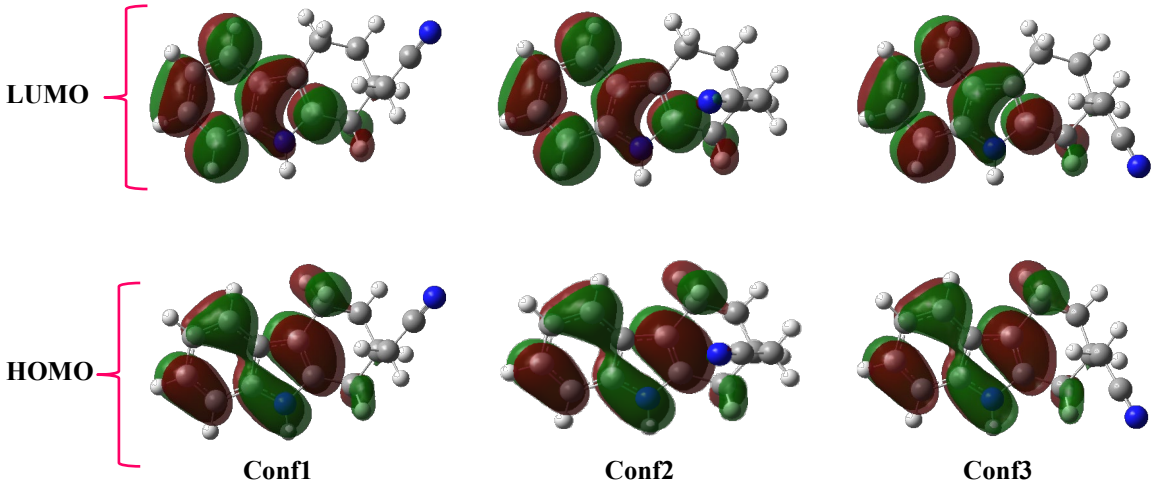

Fig. 4. HOMO and LUMO visualizations of the three stable conformers for the B3LYP/6-311++G(d,p)level in the water phase (isoval:0.02).

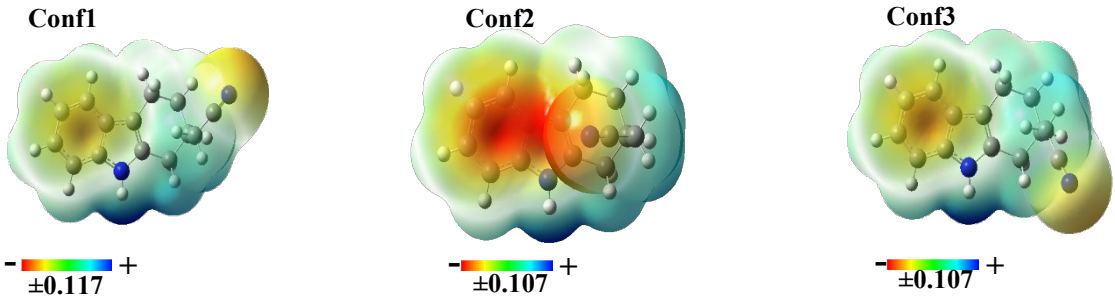

Fig. 5. The total electron density surface with ESP for the three stable conformers for using the 6-311++G(d,p) basis set in the water phase (Iso value:0.0004)

Vibrational analysis

Table 5 shows the selected vibrational modes of the studied compound obtained by FT-IR and simulated by the DFT method. The simulated frequencies for the stable conformers were scaled down by using a scaling factor of 0.9668 [24] for B3LYP/6-311++G(d,p) level of the theory to further match the vibrational mode values to the corresponding experimental values. The potential energy distribution (PED) analysiswas employed to assign the vibrational frequencies of Conf3 and to verify them by the GaussView 6.0 package. The selected vibrational modes of each stable conformer of the studied compound and corresponding observed values are given in Table 5.

As it is well known, the N-H stretching and out-of-plane N-H bending (opb N-H) vibrational modes are very good wavenumbers to predict the functional groups of the specific molecular system but the in-plane N-H bending (ipb N-H) mode may not be good to predict wavenumber because it can be variable in the IR spectrum in terms of the location and intensity. It is well known that the N-H stretching band for the secondary amines occurs in the range 3500-3300 cm^{-1}[32]. In addition, the ipbH-N modes contaminated by the other modes, especially the ring vibrational modes, were in simulated in the range 1218- 1221 cm^{-1} by DFT methodat observed in 1221 cm^{-1}[33].In addition, the opbH-N bending modes were found out at 483 and 435 $cm^{-1}$by FT-IR and calculated in the range 486-358 cm^{-1} by the DFT method [33]. In our previous study, the N-H stretching mode was recorded at 3230 cm^{-1} and simulated at 3523 $cm^{-1}$by HF method (chloroform phase) for the substituted carbazole compound [12]. In this work, we have observed the N-H stretching mode at 3268 cm^{-1} and simulated at 3525 cm^{-1} (Conf3) by DFT method. It can be noticed from Table 5 that the in-plane N-H bending modes were calculated as a mixed mode with in-plane bending ring vibrations and predicted between 1599- 1186 cm^{-1} by the DFT method. On the other hand, the out-of-planeH-N bending frequencies were calculated between 630-389 cm^{-1} by DFT method and this band was also predicted as a mixed mode with out-of-plane ring vibrations. The N-C stretching mode for the nitrile group of the studied compound was computed at 2257 cm^{-1} (91% PED) and observed at 2165 cm^{-1}.

As it is expected from literature data, the C-C stretching modes for the aromatic rings of the compound have been observed in the range 1607-1242 cm^{-1} and simulated in 1599-1280 cm^{-1} by DFT.

Here, it is important to note that C-C stretching modes for the aromatic ring were generally as a mixed mode with the aromatic ring bending modes such as in-plane H-N and C-H bending modes. In addition, the symmetric and asymmetric C-H stretching vibrations in the aromatic ring for the Conf3 were simulated at 3081 cm^{-1} (94%, PED) and in the range 3071-3054 cm^{-1}, respectively. On the other hand non-aromatic ring and aliphatic C-H stretching modes for Conf3 were calculated in the range 2966-2947 cm^{-1}.

The non-aromatic ring bendingmodes for Conf3 were calculated in the range 1444-1418 cm^{-1}(scissoring, σCH2), 1357-1299 cm^{-1} (wagging, ωCH2), 1247-1142 (rocking, ρCH2), 960-844 cm^{-1} (twisting, τCH2) respectively. It is important to keep in mind that Table 5 shows a selection of of both observed and calculated results. It is clear that, as expected, the CH2 bending modes decreased in the following order: σ CH2 > ω CH2 > τ CH2 > ρ CH2 according to the wavenumber.

^{13}C and ^{1}H NMR spectral studies

NMR spectroscopy as an analytical technique is used in many kinds of research fields to estimate the molecular structure and the molecular conformation in solution when the basic structure is known in addition to studying content and purity. Table 6 shows the ^{13}C and ^{1}H NMR chemical shifts for the three stable conformers of the studied compound.

Table 5. Selected observed and calculated vibrational frequencies (in cm^{-1}) of the studied compound in the water phase at B3LYP/6-311++G(d,p) level.

	Conf1			Conf2			Conf3			PED % (Conf3)
Exp.	Unscal.	Scal.	I_{IR}	Unscal.	Scal.	I_{IR}	Unscal.	Scal.	I_{IR}	
3268	3645	3524	140	3645	3524	138	3646	3525	139	$\nu N_{23}H$ **(100)**
	3187	3081	32	3186	3081	32	3187	3081	32	νCH R**A(94)**
	3176	3071	49	3176	3071	50	3176	3071	49	ν_{as}CH R**A(92)**
	3088	2986	10	3079	2977	5	3089	2986	10	$\nu_{as}C_{26}H2$ **(95)**
	3069	2967	65	3064	2962	79	3068	2966	70	$\nu_{as}C_{14}H2$ R**C (92)**
	3049	2948	12	3041	2940	15	3048	2947	13	$\nu C_{26}H2$ **(87)**
	3046	2945	27	3040	2939	11	3046	2945	27	$\nu_{as}C_{12}H$ R**C (89)**
2925	2990	2890	73	3000	2900	70	2991	2892	71	$\nu C_{15}H$ R**C (95)**
2165	2335	2257	80	2333	2255	57	2335	2257	81	$\nu N_{30}C$ **(91)**
1607	1654	1599	13	1655	1600	15	1654	1599-1465	12	νCC R**AB (60)**+ ipb $HN_{23}C$
1455	1495	1445	8	1494	1444	9	1494	1444-1418	7	σ CH2 R**C (73)**
1396	1459	1411	11	1455	1406	22	1458	1410	16	σ $C_{26}H2$ **(56)**
	1404	1357	13	1405	1358	10	1404	1357	13	ω CH2 R**C**+ ipb $HN_{23}C$ **(71)**
1319	1360	1315	42	1360	1315	50	1359	1314	58	νCC R**AB**+ ω CH2 R**C(69)**
	1327	1283	36	1328	1284	59	1324	1280	39	νCC R**AB**+ ω CH2 R**C (34)**
1242	1289	1246	11	1295	1252	41	1290	1247	8	τ CH2 R**C (54)**
	1261	1219	5	1271	1229	13	1275	1232	3	τ CH2 R**C (50)**
	1256	1214	32	1254	1212	23	1255	1213	32	ipb HCC R**A (43)**
	1231	1190	3	1234	1193	1	1226	1186	6	ipb $HN_{23}C$ **(43)**
	1222	1181	5	1225	1184	6	1212	1172	2	τ $C_{26}H2$ **(68)**
	1189	1150	4	1196	1156	1	1200	1161	1	τ CH2 R**C (52)**
1131	1170	1131	14	1172	1133	13	1170	1131-995	13	ipb HCC R**A (64)**
979	983	950	2	990	957	3	993	960	6	ρ CH2 R**C (53)**
930	948	916	2	941	910	4	942	942-723	3	opb HCC R**A (91)**
655	652	630	17	665	643	6	652	630-389	16	opb $HN_{23}C$ **(59)**

The PED results are given for Conf3 (most stable structure). $I_{IR,}$ IR intensity, The abbreviations are: ν, symmetric stretching; $\nu_{as,}$ asymmetric stretching; ω, wagging; τ, twisting; ρ, rocking; σ, scissoring; ipb, in-plane bending; opb, out-plane bending; R, ring.

In the past, the ^{13}C NMR chemical shifts for the C atoms in the aromatic ring were found in the range 114-143 ppm and simulated in the range 112-146 ppm, by B3LYP/6-311++G(d,p) level of the theory, in the gas phase [34]. In the literature, it was reported that ^{13}C NMR shifts for the C atoms in the non-aromatic ring were observed in the range 25-48 ppm in DMSO-$_{d6}$ and simulated in the range 26-56 ppm by B3LYP/631G(d) level of the theory [35]. In this paper, the 13C NMR chemical shifts for the aromatic and non- aromatic rings for Conf3 were recorded in the range 108.9-135.9 ppm and in the range 19.3-32.1 ppm, respectively, and computed in the range 115.7-143.3 and 21.2-38.1 ppm (gas phase). It is worth noticing that ^{13}CNMRchemical shift for the C27 is observed at 118.1 ppm and calculated at 129.7 ppm (Conf3) in the water phase.

On the other hand, the ^{1}H NMR chemical shifts of the aromatic and non-aromatic ring for the substituted benzimidazole hydrate compound were recorded in the range 7.22-7.89 [34] and 1.5-1.8 ppm [35] whereas they were simulated in 7.35-7.85 ppm [34] and 1.5- 1.8 ppm by the DFT method [35]. In this work, the ^{1}H NMR chemical shifts of the aromatic and non-aromatic rings for Conf3 were observed in the range 7.24-7.78 and 1.78-2.94 ppm, whereas they have been computed in the 7.35-7.76 and 1.99-3.21 ppm by the DFT method (water). It is clear that the chemical shift values of the hydrogen atoms closer to the electronegative atom are higher than the chemical shift values of the other hydrogen atoms.

Last, the linear regression analysis for both the ^{13}C and ^{1}H NMR chemical shifts was employed to show the relationship between the observed and calculated chemical shifts; the regression equations are given in Table 7. Accordingly, the best correlation coefficient between the observed and simulated ^{13}C NMR chemical shifts is determined as R^2= 0.9992 (with the std. err. S= 1.3887) for Conf2 (gas) while the best correlation coefficient between the observed and calculated ^{1}H NMR chemical shifts is found to be R2= 0.9967 (with the std. err. S= 0.2564) for Conf3 (gas). These results indicate that the simulated ^{13}C and ^{1}H NMR chemical shifts agree with the corresponding observed values.

Table 6. The observed and calculated ^{1}H and ^{13}C NMR isotropic chemical shifts (in ppm) for the studied compound, at 6-311++G(d,p) basis set.

		Gas phase			Water phase		
^{13}C	*Exp.*	Conf1	Conf2	Conf3	Conf1	Conf2	Conf3
1C	119.3	126.1	125.7	126.0	124.8	124.7	124.8
2C	121.4	128.1	127.8	128.0	126.5	126.5	126.5
3C	108.9	114.4	114.3	114.7	115.7	115.7	115.7
4C	135.9	143.2	143.4	143.2	143.3	143.3	143.3
5C	127.4	134.7	134.8	134.6	134.8	134.7	134.8
6C	118.9	123.5	123.6	123.0	122.9	122.9	122.9
11C	131.6	135.6	135.5	136.5	140.1	140.7	140.0
12C	28.9	33.5	30.8	30.2	32.9	30.4	30.3
13C	32.1	37.6	36.6	38.1	37.0	35.7	37.6
14C	28.1	29.1	34.1	33.0	29.2	33.2	32.6
15C	19.3	20.5	22.1	21.2	20.4	22.0	20.8
16C	111.2	116.3	118.0	114.6	114.9	116.8	114.8
26C	22.8	21.9	25.7	21.8	21.2	24.4	21.3
27C	118.1	123.2	122.3	123.8	129.2	129.3	129.7
^{1}H	*Exp.*	Conf1	Conf2	Conf3	Conf1	Conf2	Conf3
7H	7.24	7.31	7.27	7.29	7.35	7.35	7.35
8H	7.34	7.32	7.31	7.33	7.38	7.39	7.38
9H	7.45	7.30	7.30	7.34	7.59	7.61	7.60
10H	7.78	7.67	7.64	7.61	7.78	7.78	7.76
17H	2.94	3.23	3.28	3.08	3.29	3.35	3.21
18H	1.78	2.49	1.99	1.85	2.33	2.15	1.99
19H	2.79	2.89	2.91	2.87	2.93	2.98	2.88
20H	2.61	2.84	3.25	2.66	2.85	3.10	2.72
21H	2.79	2.30	2.65	3.02	2.58	2.85	3.00
22H	2.19	1.91	2.12	2.05	2.02	2.14	2.08
24H	7.17	6.92	6.99	7.07	7.72	7.81	7.80
25H	2.54	2.41	2.20	2.41	2.58	2.47	2.57
28H	2.54	2.10	2.38	2.48	2.45	2.62	2.56
29H	2.42	2.52	2.55	2.11	2.59	2.82	2.43

Table 7. Regression equations between observed and calculated *^{1}H* and*^{13}C* NMR shifts of the studied compound at B3LYP/6-311++G(d,p) level.

Method/ phase	Conformer	*^{13}C*	*^{1}H*
B3LYP/ gas	Conf1	δ_{exp}= 0.9618δ_{calc} -1.0410 (R^2= 0.9989. S= 1.6820)	δ_{exp}= 1.0098 δ_{calc}- 0.0151 (R^2= 0.9836. S= 0.3260)
	Conf2	δ_{exp}= 0.9759δ_{calc} -2.8283 (R^2= 0.9992. S= 1.3887)	δ_{exp}= 1.0258 δ_{calc}-0.1288 (R^2= 0.9899. S= 0.2564)
	Conf3	δ_{exp}= 0.9650δ_{calc} -1.4070 (R^2= 0.9987. S= 1.8087)	δ_{exp}= 1.0074 δ_{calc}-0.0022 (R^2= 0.9967. S= 0.1472)
B3LYP/ water	Conf1	δ_{exp}= 0.9492δ_{calc} -0.2385 (R^2= 0.9981. S= 2.1757)	δ_{exp}= 0.9848 δ_{calc}-0.0659 (R^2= 0.9912. S= 0.2387)
	Conf2	δ_{exp}= 0.9579δ_{calc} -1.5430 (R^2= 0.9986. S= 1.8600)	δ_{exp}= 0.9972 δ_{calc}-0.1905 (R^2= 0.9919. S= 0.2294)
	Conf3	δ_{exp}= 0.9522δ_{calc} -0.6637 (R^2= 0.9978. S= 2.3433)	δ_{exp}= 0.9786 δ_{calc}-0.0313 (R^2= 0.9952. S= 0.1762)

CONCLUSIONS

In summary, we have completed divergent and efficient routes for the synthesis of 2-(2,3,4,9,-tetrahydro-1*H*-carbazol-2-yl)acetonitrile. This method could be extended to the syntheses of other alkaloids. Finally, we believe that congeners of the nitrile **3** will become versatile starting materials for the synthesis of diverse alkaloids bearing carbazole units.The PES scan carried out in the gas phase by the DFT method revealed three stable conformers that are very close to each other in terms of the energy. NBO analysis indicated that the resonance interactions (π→π* and n→π*) for all stable

conformers have mainly contributed to the lowering of the molecular stability. The pictorial representation of HOMO shows that the nucleophilic attack site is around the aromatic ring (partly non-aromatic ring) of each stable conformer. Also, we have observed the NMR and FT-IR spectra of the studied compound and compared each of them with the computational results we have performed. This study has shown that the observed and simulated spectroscopic results are in good agreement with each other.

Acknowledgements: *This work was financially supported by the Scientific and Technological Research Council of Turkey (TUBITAK Project No.112T503) and Sivas Cumhuriyet University Scientific research projects department (Project No: CUBAP: EĞT-072). All simulations have been carried out at TUBITAK ULAKBIM, High Performance and Grid Computing Center (TR-Grid e-Infrastructure).*

REFERENCES

1. T. Kametani, T. Suziki, *J. Chem. Soc.C*, 1053 (1971).
2. J.Diez, P.Castells, M.Forns, D.Rubiralta, S. Grierson, H.-P. Husson, X. Solons, M. Font-Bardia, *Tetrahedron*, **50**, 6585 (1994).
3. C.Seide, A. De Moraes Santos, A. De Simone, M. Bartolini, A. M. Weffort-Santos, V. Andrissano, *Curr. Alzheimer. Res*., **14**, 317 (2017).
4. H. Baggio, G. De Martini Otofujı, W. M. Souza, C. A. De Moreas Santos, L. M. Torres, L. Rieck, M. C. De Andrade Marques, S. Mesia-Vela, *Planta Med.,***71**, 733 (2005).
5. J. M. Nardin, W. M. De Souza, J. F. Lopes, A. Florao, C. A De Moreas Santos, A. M. Weffort-Santos, *Planta Med*., **74**, 1253 (2008).
6. F. Tang, M. G. Banwell, A. C. Willis, *J. Org Chem*., **81**, 2950 (2016).
7. M.Amat, M. Perez, N. Llor, M, Martinelli, E. Mollins, *J. Chem. Commun*., **14**, 1602 (2004).
8. S. Patir, N. Uludag, *Tetrahedron*, **65**, 115 (2009).
9. N. Uludag, R. Yılmaz, O. Asutay, N. Colak, *Chem. Heterocycl. Compd.*, **52**, 196 (2016).
10. N. Uludag, M. Sanda, O. Asutay, N. Coskun, *Org. Prep. Proc. Int*., **46**, 551 (2014).
11. N. Uludag, M. Yakup, *Org. Prep. Proc. Int*., **47**, 454 (2015).
12. N. Uludag, G. Serdaroglu, A. Yinanc, *J. Mol. Struct*., **1161**, 152 (2018).
13. G. Serdaroglu, N. Uludag, *J. Mol. Struct*., **1166**, 286 (2018).
14. T.A. Reekie, M.G. Banwell, A.C. Willis, *J. Org. Chem.,* **77**, 10773 (2012).
15. N. Uludag, G. Serdaroglu, *J. Mol. Struct*., **1155**, 548 (2018).
16. A. D. Becke, *J. Chem. Phys*., **98,** 1372 (1993).
17. C. Lee, W. Yang, R. G. Parr, *Phys. Rev*., **B37,** 785(1988).
18. J. B. Foresman, T. A. Keith, K. B. Wiberg, J. Snoonian, M. J. Frisch, *J Phys. Chem*., **100**, 16098 (1996).
19. J. Tomasi, B. Mennuci, R. Cammi, *Chem. Rev*.**, 105**, 2999 (2005).
20. F. Weinhold, C. R. Landis, E. D. Glendening,*Int. Rev. in Phys. Chem.,* **35,** 399 (2016).
21. A.E. Reed, L.A. Curtiss, F. Weinhold,*Chem. Rev.,* **88,**899 (1988).
22. M. Rohlfing, C. Leland, C. Allen, R. Ditchfield, *Chem. Phys*., **87**, 9 (1984).
23. K. Wolinski, J.F. Hinton, P. Pulay,*J. Am. Chem. Soc*.,**112 (23),** 8251 (1990).
24. G. Shakila, H. Saleem, N. Sundaraganesan, *World Scientific News*, **61(2),** 150 (2017).
25. M. H. Jamroz, Vibrational Energy Distribution Analysis VEDA 4, Warsaw, (2004-2010).
26. M. J. Frisch, G. W. Trucks, H. B. Schlegel, G. E. Scuseria, M. A. Robb, J. R. Cheeseman, G. Scalmani, V. Barone, B. Mennucci,G. A. Petersson, H. Nakatsuji, M. Caricato, X. Li, H. P. Hratchian, A. F. Izmaylov, J. Bloino, G. Zheng, J. L. Sonnenberg, M. Hada, M. Ehara, K. Toyota, R. Fukuda, J. Hasegawa, M. Ishida, T. Nakajima, Y. Honda, O. Kitao, H. Nakai, T. Vreven, J. A. Montgomery, Jr.,J. E. Peralta, F. Ogliaro, M. Bearpark, J. J. Heyd, E. Brothers, K. N. Kudin, V. N. Staroverov, T. Keith, R. Kobayashi, J. Normand, K. Raghavachari, A. Rendell, J. C. Burant, S. S. Iyengar, J. Tomasi, M. Cossi, N. Rega, J. M. Millam, M. Klene, J. E. Knox, J. B. Cross, V. Bakken, C. Adamo, J. Jaramillo, R. Gomperts, R. E. Stratmann, O. Yazyev, A. J. Austin, R. Cammi, C. Pomelli, J. W. Ochterski, R. L. Martin, K. Morokuma, V. G. Zakrzewski, G. A. Voth, P. Salvador, J. J. Dannenberg, S. Dapprich, A. D. Daniels, O. Farkas, J. B. Foresman, J. V. Ortiz, J. Cioslowski, and D. J. Fox, Gaussian 09 D.01. Gaussian, Inc, Wallingford CT (2013).
27. ChemOffice17 suite, Perkin Elmer, 2017.
28. GaussView6.0, Gaussian, Inc, Wallingford CT, 2016.
29. S. Murugavel, P. S. Kannan, A. SubbiahPandi, T. Surendirand, S. Balasubramaniane, *Acta Crystallogr. E,* **64**, o2433 (2008).
30. K. Fukui, *Scienc*e, **218,4574,** 747 (1982).
31. R. G. Parr, L. V. Szentpaly, S. Liu, *J. Am. Chem. Soc*., **121**, 1922 (1999).
32. T. Kavitha, G. Velraj, *J. Mol. Struct*., **1141**, 335 (2017).
33. H. Singh, S. Singh, P. Agarwal, P. Tandon, R. D. Erande, D. H. Dethe, *J. Mol. Struct*., **1153**, 262 (2018).
34. Y. E. Bakri, E. H. Anouar, Y. Ramli, E. M. Essassi, J. T. Mague, *J. Mol. Struct.***, 1152**, 154 (2018).
35. N. B. Arslan, C. Kazak, F. Aydın, *J. Mol. Struct.,* **1155**, 646 (2018).

ОТНОСНО СИНТЕЗА НА АЛКАЛОИДИ ОТ УЛЕИНОВ ТИП ЧРЕЗ ФИШЕРОВА РЕАКЦИЯ НА ИНДОЛОВ СИНТЕЗ: FT-IR, NMR СПЕКТРОСКОПСКО И ИЗЧИСЛИТЕЛНО ИЗСЛЕДВАНЕ НА ЗАМЕСТЕНО КАРБАЗОЛОВО СЪЕДИНЕНИЕ

Г. Сердароглу[1], Н. Улудаг[2*]

[1]Сивас Университет Джумхуриет, Департамент по наука и образование, 58040, Сивас, Турция
[2]Университет Намик Кемал, Департамент по химия, 59030, Текирдаг, Турция

Постъпила на 1 юли, 2018 г.; приета на 1 октомври, 2018 г.

(Резюме)

Представен е ефективен директен метод за синтез на 2-(2,3,4,9-тетрахидро-1*H*-карбазол-2-ил) ацетонитрил чрез Фишерова реакция между фенилхидразин хидрохлорид и 2-(3-оксоциклохексил) ацетонитрилв присъствие на етанол. Предимства на тази процедура са меките реакционни условия, добрите добиви на реакционните продукти, краткото време на реакцията и простотата на изпълнение. Повърхността на потенциалната енергия е сканирана за определяне на стабилните конформери на изучаваното съединение в газова фаза на ниво B3LYP/6-31G(d,p) на теорията. Наблюдавани са ^{1}Hи^{1}C NMR химични отмествания за всеки стабилен конформер, които са симулирани чрез DFT метода в газова и водна фаза. Регистрираният FT-IR спектър на изучаваното съединение е сравнен със симулираните вибрационни режими за всеки стабилен конформер. NBO е използван за предсказване на важни междумолекулни взаимодействия, допринасящи за понижаване на молекулната енергия на стабилизация на всеки стабилен конформер. FMO анализ и MEP диаграми са използвани за предсказване на физикохимичните и квантово-химични параметри за оценка на химичната реактивоспособност и реактивните центрове на всеки стабилен конформер.